Journal of Chromatography A, 1216 (2009) 3423–3430

Contents lists available at ScienceDirect

Journal of Chromatography A

journal homepage: www.elsevier.com/locate/chroma

Ultraviolet thermal lensing detection of amino acids

Fang Yu [a], Alexander A. Kachanov [a,b], Serguei Koulikov [b], Ann Wainright [b], Richard N. Zare [a,*]

[a] Department of Chemistry, Stanford University, Stanford, CA 94305-5080, USA
[b] Skymoon Ventures, Santa Clara, CA 95054, USA

ARTICLE INFO

Article history:
Available online 17 June 2008

Keywords:
Optical detection system
Amino acids
Thermal lensing

ABSTRACT

Thermal lensing (TL) permits ultra-sensitive measurements of optical absorption of analytes in very small liquid volumes. We report the construction and use of a TL detector based on pulsed ultraviolet (UV) laser excitation (266 nm). We applied this detector to quantitate amino acids using capillary electrophoresis (CE) as a means of separation. Sixteen individual amino acids are readily detected, but the signal has a complex dependence on intensity caused by the combination of (1) one-photon absorption; (2) two-photon absorption (TPA); and (3) photodestruction of amino acid molecules in the focus of the laser beam. An aqueous solution containing tyrosine, tryptophan, and cysteine is electrophoretically separated and the individual amino acids are detected by UV TL. The estimated limit of detection is 7 μM for tyrosine, 2.5 μM for tryptophan and 33 μM for cysterine, which translates into 0.35 fmol for tyrosine, 0.125 fmol for tryptophan, and 1.65 fmol for cysteine in the 140 pL detection volume. It is found that two-photon absorption of water and the formation of color centers in the fused silica walls of the flowcell can contribute a significant, drifting background signal, but this interference can be minimized by selecting an appropriate focus condition and excitation–detection geometry. We suggest that as UV laser sources become available, UV TL may become a method of choice for measuring the concentrations of many analytes in different separation formats in which the volume is highly limited.

1. Introduction

The miniaturization of analytical devices is seriously challenging detection technology. In particular, conventional UV–vis absorbance measurements are becoming increasingly difficult for detecting analytes in extremely small sample volumes, such as encountered in capillary electrophoresis (CE), microcolumn high performance liquid chromatography (HPLC), or microfluidic devices. When possible, laser induced fluorescence (LIF) detection is frequently used in the abovementioned applications to offer ultra-high sensitivity, but LIF only detects fluorescent molecules. For nonfluorescent species, LIF detection requires an extra derivatization step, which is time-consuming and potentially detrimental to separation and quantification. For many small molecules, the derivatization chemistry may be problematic.

Thermal lensing (TL) technology may be a promising alternative [1–4]. TL has a long history being applied to actual separations [5,6]. TL detects a change of the refractive index induced by local heating that results from optical absorption of a laser beam (excitation beam) focused within the small volume of the liquid sample. To achieve better sensitivity, a separate laser (probe beam) is used to monitor the lensing effect. TL is based on light absorbance and therefore inherits the 'label-free' advantage of UV–vis absorption detection. The sensitivity that TL can offer has been demonstrated to be extraordinary in the visible. In a side-by-side comparison reported by us [7], TL shows 140 times better sensitivity than a state-of-art commercial UV–vis detector. TL is well suited for the detection of analytes in short-path-length devices at ultralow cell volumes with no penalty in minimum detectable concentration.

The "thin TL" theory of Shen et al. [8] can be used to predict the magnitude of the TL signal with relatively good accuracy and versatility. Their expression for the absolute value of a small TL signal for an excitation beam modulation period much longer than the temperature relaxation time of the sample medium can be written as,

$$\frac{I(t)}{I_0} = \theta \tan^{-1}\left(\frac{2mV}{[(1+2m)^2+V^2](t_c/2t)+1+2m+V^2}\right), \quad (1a)$$

where

$$\theta = \frac{P_e\, dn/dT}{\kappa\lambda_p}\alpha L, \quad (1b)$$

P_e is excitation power, dn/dT is the temperature derivative of the refractive index of the medium, κ is the thermal conductivity, α

* Corresponding author. Tel.: +1 650 7233062; fax: +1 650 7250259.
E-mail address: zare@stanford.edu (R.N. Zare).

0021-9673/$ – see front matter © 2008 Elsevier B.V. All rights reserved.
doi:10.1016/j.chroma.2008.05.096

is the absorption coefficient, and L is the length of the absorbing layer. αL then is the fraction of the excitation power absorbed in the medium. The factor in front of αL is a scaling coefficient between a TL measurement and an ordinary absorption measurement, and it is known as the "thermal lens enhancement factor". The parameter t_c gives the time dependence of the probe beam intensity, and it is called a thermal time constant, related to the excitation beam waist size and the thermal diffusivity of the medium. The m and V are the probe/excitation beam size mismatch and the position mismatch parameters, respectively. Eq. (1) has been derived for a "thin thermal lens" case when both the probe beam and excitation beam sizes have small variations within the probe volume. However, in our recent study [7] we found that Eq. (1) can give as well fairly good predictions of the thermal lens signal in the case of tight focusing of the beams. In the case of a TL experiment with equal excitation and probe beam waists, Eq. (1) simplifies to $\Delta I/I_0 = \theta\alpha L$. For this reason θ is often called a "thermal lens enhancement factor" [9] as in this simple case θ expresses how much larger or smaller the relative variation of the probe beam is compared to attenuation of the beam at the measurement wavelength caused by linear absorption. A useful number to remember is that with a He–Ne laser at 632.8 nm as a probe and the excitation beam power of 4.2 mW in water, $\theta = 1$.

Most reported TL applications use continuous-wave (CW) light sources in the visible. For broader TL applications, a UV excitation laser is desired for the direct detection of various 'colorless' molecules without labeling. Only a few reports on UV laser-based TL for label-free detection can be found in the literature. Waldron and Dovichi [10] used a low-energy krypton fluoride laser to detect 20 phenylthiohydantoln derivatized amino acids separated by micellar capillary electrophoresis. Following this, people have used the similar detection principle to analyze products from manual peptide sequencing [11], food preservatives [12] and tricyclic antidepressants [13]. Krattiger et al. [14] used a frequency-doubled argon ion laser at 257 nm for the detection of various nucleoside and mono- and diphosphate nucleotide mixtures. Ragosina et al. [15] reported a crossed-beam TL sensor with CW 257 nm laser excitation and applied it to capillary electrophoresis detection of nitroaromatic compounds. They reported that the sensitivity was 30 times higher than that with a UV spectrophotometer. Kitamori and co-workers [16] reported a TL microscope with a pulsed UV excitation laser for the detection of nonfluorescent molecules and claimed two orders of magnitude higher sensitivity than that of a spectrophotometric method.

There are some special challenges in the development of the TL technique in the UV. First of all, the availability of UV lasers is limited. Most 'colorless' molecules have their absorption bands in the deep UV range (<300 nm). The most common sources in this range are excimer lasers, but they operate in pulsed mode with low repetition rates, which is not well-suited for TL. Argon ion lasers with intra-cavity second harmonic generation (SHG) crystals can provide deep CW UV radiation, but both excimer and ion laser size and power consumption requirements make them not acceptable in practical analytical instrumentation. The second challenge is that the power of UV lasers is usually not high enough, especially for CW sources based upon frequency doubling or mixing. According to Eq. (1), when water is used as a solvent and a He–Ne laser as a probe, the TL signal becomes lower than the signal in ordinary absorption at an excitation beam power less than 4.2 mW. Third, in the deep UV range, the absorption (linear and two-photon) of the solvent and flow cell materials may lead to background signal causing the signal-to-noise ratio (SNR) to decrease, especially when the UV source has large power fluctuations. Fourth, the choice of solvents becomes increasingly limited in the deeper UV range owing to the solvent's UV absorbance.

Perhaps, one of the most versatile and cost-effective ways to generate coherent UV radiation is to use a pulsed laser with subsequent harmonic generation crystals for frequency conversion.

A very promising way to generate deep UV radiation in a very compact low-cost system is nonlinear frequency conversion of a high repetition rate passively Q-switched microchip solid-state laser [17]. Such lasers can operate at repetition rates approaching 100 kHz with average powers in the fundamental of a few hundred milliwatts. These characteristics make them equivalent to CW lasers for TL detection because thermal relaxation is a rather slow process compared to such rates, even with small detection volumes. The nanosecond to sub-nanosecond pulse duration of such lasers results in peak optical powers approaching 10 kW. We can expect therefore a very high conversion efficiency for fourth harmonic generation of 266 nm, or even fifth harmonic generation at 213 nm.

We designed and tested a UV TL setup using a solid-state 33 kHz – repetition rate Q-switched Nd:YAG frequency-quadrupled microchip laser operating at 266 nm. The detection of amino acids was investigated as a model system. Amino acid analysis [18,19] is an important methodology to determine the amino acid composition or content of proteins, peptides, and some pharmaceutical preparations. Usually, methods used for amino analysis are based on an electrophoretic or chromatographic separation. However, in conventional amino acid analysis, amino acid constituents of the test sample are derivatized with chromophores or fluorophores prior to analysis. Here, we directly detect amino acids by UV-excited TL and explore the separation and TL detection of several amino acids by CE.

2. Experimental

2.1. Chemicals

All test solutes are used as received without further purification. The amino acids were from Sigma-Aldrich (L-amino acids LAA21-1KT) and the stock solutions of the amino acids were prepared in 10 mM borate buffer (sodium tetraborate decahydrate, 419450010 (Acros Organics)). The separation buffers were prepared from sodium tetraborate and NaOH to obtain the desired pH. All water used was freshly obtained from the Millipore System (resistance > 18 MΩ).

2.2. Thermal lensing setup

Fig. 1 shows the TL setup. The excitation source consists of a microchip Nd:YAG laser operating at 1064 nm and two crystals, 20 mm long potassium titanyl phosphate (KTP) for frequency doubling and 30 mm long deuterated potassium dihydrogen phosphate (DKDP) for obtaining the fourth harmonic at 266 nm. The microchip laser emits 20 μJ pulses of 670 ps duration at a repetition rate of ~33 kHz. Its output beam is focused between the two closely spaced nonlinear crystals with a lens having a focal length of 200 mm. High peak fluence of such pulses results in UV output at the excitation wavelength of $\lambda_e = 266$ nm with an average power of about 10 mW. The fourth harmonic is separated from the lower-order harmonics by a Pellin–Broca fused silica prism. The divergence of the UV beam is 11.3 mrad, which arises from the focusing lens. A beam splitter prism is used to direct a portion of the UV power to a slow-response photodiode (time constant = 1 s) as a reference signal to monitor average UV power and take into account its changes in time from temperature drifts. The laser passes through a mechanical chopper with a modulation frequency of typically 300 Hz.

In the experiment, we tested three different focus conditions for the UV beam, namely loose, moderate, and tight focusing. Loose

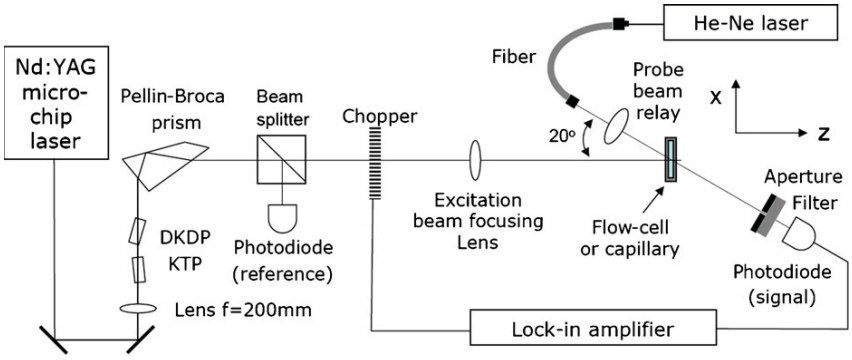

Fig. 1. Experimental setup for UV thermal lensing.

focusing is achieved by a 100 mm plano-convex singlet lens with the UV beam diameter at the lens of 1.3 mm. For moderate focusing, the same 100 mm singlet is used with the entrance UV beam diameter increased to 3.2 mm. For tight focusing, a three-element lens designed in accordance with Melles Griot suggestions [20] is used to form an aberration–corrected lens with an effective focal length of 18.6 mm and back focal length of 35.1 mm.

The probe beam source is a low-noise 0.5 mW He–Ne laser (Melles Griot) operating at a wavelength of $\lambda p = 632.8$ nm with the output beam diameter and divergence angle at the $1/e^2$ level of 0.63 mm and 1.3 mrad, respectively. The probe laser is coupled to a single-mode fiber (Thorlabs APC patch cord P3-630A-FC-5) with the mode-field diameter of 4.3 μm, and the fiber output is relayed into the sample using a pair of lenses with 4× magnification. The probe beam crosses the excitation beam at an angle of 20° and hits the photodetector. The detector signal is an amplified using a switchable-gain silicon photodiode (model PDA55, Thorlabs) with five gain settings. A narrow band-pass filter centered at the probe beam wavelength and a pinhole are placed in front of the photodiode, as is common in TL experiments. The signal from the photodiode is processed by a lock-in amplifier (model SR830, Stanford Research Systems). The time constant of the lock-in amplifier in all measurements was 300 ms, and the filter slope was 24 dB/octave. The lock-in amplifier extracts the signal at the reference frequency and outputs it as a digital signal which is transferred to a PC via GPIB. The thermal lensing signal from the photodiode and the reference frequency from the function generator are also sent to an oscilloscope to assist the alignment and signal optimization.

We used a flowcell (model 48UV0.1, NSG Precision Cells, Inc.) for optimization of the thermal lensing experimental parameters and a fused silica capillary for CE measurements. The flowcell is made of two parallel 1.25 mm thick UV-grade fused silica slabs separated by a distance $L = 100$ μm. The total volume of the cell is 30 μL. The sample is injected into the flow cell by a peristaltic pump. Typically, a linear flow rate of 4.2 mm/s is maintained in the flowcell, which is fast enough to avoid photochemical destruction of the analytes but yet does not decrease the TL response. The excitation beam focusing lens, the flowcell (or capillary), and the fiber holder were mounted on translational stages allowing micrometric adjustments, providing complete freedom in mutual adjustments of the laser beams overlap and in the location of the flowcell (or capillary) with respect to the beam waists. For making scans of the cell position in the *x*-direction, we used a motorized translation stage (Newport).

For CE experiments we used either rectangular (100 μm width) or circular (50 μm i.d.) polyimide-coated fused silica capillaries (Polymicro, Inc.). The polymer coating of the capillary was removed with heated concentrated sulfuric acid over 1 cm at the beam intersection region. The CE system is home-built. The core part is a DC–DC high-voltage generator (30A12-P4-STD) purchased from Ultravolt. The high voltage is regulated by the AUX DC output from the SR830 lock-in amplifier. The sample injection is electrokinetic. The pretreatment and rinse of capillary is done at a pressure of ~2 psi.

3. Results and discussion

3.1. UV beam profile measurement

In a TL experiment it is important to know the profiles of both the excitation and the probe beams, because they determine the magnitude of the TL signal. This information can be obtained in a straightforward manner with the probe beam emerging from a single-mode fiber. The parameters of this Gaussian beam can be found using elementary equations for Gaussian beam propagation. In contrast, this task is significantly more difficult for the pulsed UV beam. The walk-off in the doubling crystals makes the UV beam non-Gaussian, so that we cannot directly apply equations of Gaussian beam optics, but we need to measure its cross-section at different locations. The rotating-blade beam profilers also cannot be used with the pulsed laser. We developed a simple technique based on a general-purpose CCD camera connected to a computer. Many optical glasses have very strong absorption at 266 nm, such that the UV beam is absorbed within a few micrometers from the surface, and in addition to that they have visible fluorescence. One example of such glass is a microscope slide. The fluorescence spot thus replicates the intensity distribution of the UV beam. We reimaged this fluorescent replica into a Lumenera USB CCD camera, Model "Infinity 2-1". By moving the camera with the slide along the beam axis around the focal region we could determine from the digitized images the beam dimensions in the vertical and horizontal directions.

We have chosen the distance between the fourth harmonics crystal and the pump lens such that the beam dimensions on the pump lens were approximately equal. As a result the focused beam was nearly circular with an ellipticity of only a few percent and its profile was close to a Gaussian shape regardless of the walk-off inside the crystal. The spot sizes within the cell for all three focusing regimes are shown in Fig. 4. From these plots the beam sizes for three focusing regimes are: loose focus – 19 μm; moderate focus – 9.2 μm; tight focus – 6.2 μm. The beam quality parameter M^2 was between 1.6 and 2.2.

3.2. UV-excited thermal lensing signal from water

High repetition rate short-pulse lasers are certainly beneficial for accessing the UV range by frequency conversion. However, the

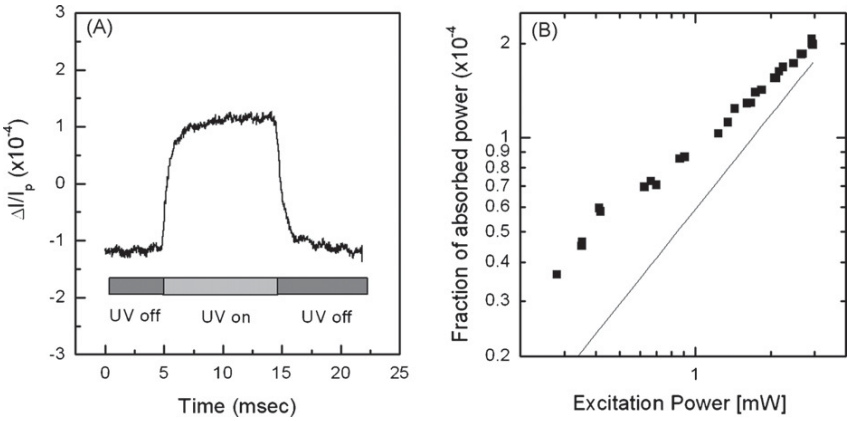

Fig. 2. (A) Representative UV TL signal under the following condition: moderate focusing, chopping frequency is 50 Hz, measured with pure water in the quartz flowcell. (B) The dependence of measured fraction of absorbed excitation power on the total excitation power for pure water sample (points) and theoretical dependence for the fraction of absorbed power due to TPA (line).

high fluence of such pulses may result in undesirable effects. Among them, TPA of the solvent may induce a high background signal and thus limit the analytical performance of TL. Kitamori and co-workers [16] observed indeed the nonlinear increase of the TL signal as a function of the excitation beam pulse energy which they attributed to TPA in water. They did not study the effect in detail, especially its impact on the detection limits. Moreover, the peak fluences in their measurements were much lower owing to higher laser repetition rates and longer pulse durations. For this reason we choose to begin by examining the nonlinear effects in water, which is a most common solvent in CE measurements.

Fig. 2(A) shows the TL signal with only pure water in the flowcell. In this measurement the chopper frequency was set to 50 Hz. The excitation radiation then consisted of 10 ms long bursts of pulses, 330 pulses per burst. The TL signal looks very similar to what one would expect from a CW excitation beam because its rise and fall time of about two milliseconds is too long for us to be able to observe in it the short 10 μs period of the pulses.

This $\Delta I/I_0 \sim 10^{-4}$ is evidently too large for linear absorption in water. The linear absorption coefficient for water at 266 nm [21] is $\alpha_{H_2O} = 5 \times 10^{-4}\,\mathrm{cm}^{-1}$. This value corresponds to an absorbed fraction of the optical power within the cell $\alpha_{H_2O}L = 5 \times 10^{-6}$, and it should have given a TL signal $\Delta I/I_0$ close to this value because the TL enhancement factor θ should be close to unity at the UV average power of a few milliwatts as can be obtained from the Eqs. (1a) and (1b). The measurements of two-photon absorption coefficient for liquid water β_{H_2O} at 266 nm have been reported in several publications, but the values vary significantly. We shall use the most recent value [22] of $\beta_{H_2O} = 49 \times 10^{-11}$ cm/W. The value for fraction of absorbed excitation power can be estimated using equation (12) from this reference as $\beta_{H_2O} I_0 L/2\sqrt{2}$, where I_0 is the intensity at the peak of the pulse. The peak intensity can be found from the pulse energy E, the beam waist w_0 and pulse duration τ as $I_0 = 4\sqrt{\ln(2)}E/\pi\sqrt{\pi}\tau w_0^2$. Such estimation for the average power of 3 mW and the beam waist radius $w_0 = 9.2$ μm gives for the absorbed fraction the value of 1.8×10^{-4} which is in reasonable agreement with TL measurements, as it is shown in Fig. 2(B). Points in this figure are obtained from measured TL signal $\Delta I/I_p$ divided by the quantity

$$\frac{P_e \mathrm{d}n/\mathrm{d}T}{\kappa\lambda_p} \tan^{-1}\left(\frac{2mV}{[(1+2m)^2+V^2](t_c/2t)+1+2m+V^2}\right)$$

in order to obtain the fraction of the absorbed excitation power αL.

The line in this figure shows the fraction of the absorbed excitation power arising from TPA calculated using the data from reference [22]. We can see that there is a reasonable agreement between measured and expected values; however TL gave a somewhat stronger signal than we would expect. We think that the deviation may be caused by the UV inscription in the cell windows material (fused silica), and we shall discuss the inscription effects in the next section of the paper. An important conclusion from this

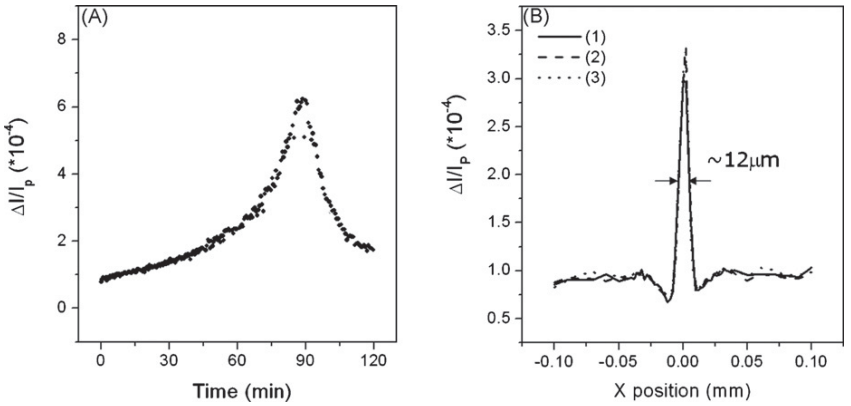

Fig. 3. (A) Typical TL baseline signal drift pattern within ~2 h, measured with pure water in the quartz flowcell. Average UV power is ~3 mW. (B) TL signal scans along x-axis (cf. Fig. 1(A)), (1) after UV inscription for ~1 h, (2) repeated as (1), (3) after sample idling for overnight.

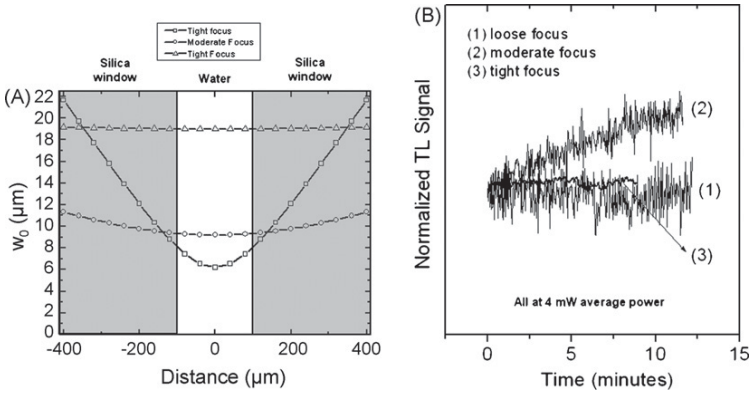

Fig. 4. (A) UV beam profiles for three different focusing conditions (see text for details). (B) Normalized UV TL baseline signal at three different focusing conditions.

measurement is that TPA from the solvent can contribute a significant background to the TL signal when a high repetition rate pulsed laser is used as UV source. This background may become a serious limiting factor in measuring small concentrations of analytes in water. The limit of detection may not be limited anymore by the shot noise in the probe beam photocurrent as it was in our recent experimental study [7] with a CW laser, but by the power fluctuations in the UV beam. In fact, for two-photon absorption, the effect of the UV beam power fluctuations will be twice as large as for linear absorption owing to the quadratic dependence of the TL signal on the UV power. In addition to that, if we recall that the UV radiation itself was obtained as a result of a two-step frequency doubling with each step quadratically dependent on the pump power, we understand that the TPA in the solvent results in very stringent requirements on the power stability of the excitation laser.

On the other hand, the analytes may have a strong TPA, and this feature can help to detect the analytes that do not possess a linear absorption at the excitation measurements. We explore this opportunity in the following sections on detecting amino acids, the majority of which have no or very weak absorption at 266 nm.

Besides, the plot in Fig. 2(A) demonstrates that two-photon absorption can be easily measured by TL, even with nanosecond pulses of rather low energy (about 10 nJ in this case), whereas for TPA measurement by direct absorption either high energy nanosecond pulses, or sub-picosecond pulses are most commonly used. Indeed, recently Ghaleb and Georges [23] measured TPA coefficients for ethanol using the TL technique.

3.3. UV inscription on fused silica

When we focused the pulsed UV beam into the UV-grade fused silica absorption cell we noticed a weak red-colored emission from UV beam track within the cell entrance and exit windows. In addition, the TL background signal with pure water exhibited quite pronounced time evolution, as shown in Fig. 3(A), where the baseline signal with pure water sample was rising in the first 1.5 h of UV illumination. During this time, the TL signal increased by a factor of ~6. Any in-plane motion of the flowcell would reset the baseline signal to the starting level (data not shown). Visual observation shows the presence of the red fluorescence induced by focused UV beam in both sides of the flowcell wall, which suggests the presence of non-bridging oxygen Hole Centers [24]. The increasing baseline signal may be caused by increasing absorbance from the flowcell walls by color center aggregation induced by high power UV irradiation. An interesting phenomenon is that after ~1.5 h of UV irradiation, the TL signal started to decrease, and within the next 30 min it went nearly down to its initial value. The visual observation shows the red fluorescence lines on both sides of the flowcell wall became asymmetrically bright, i.e., the line in the first wall that meets the laser became brighter than the second line. We do not have an explanation for this effect, but we decided not to study it in depth, because as it is discussed later in this text, the inscription effects can be reduced or even eliminated by a proper choice of the excitation beam focusing conditions. One possible explanation is that UV inscription changes the refractive index of the fused silica, and this local refractive index change may increase the divergence of the excitation beam and its diameter in the second window. The reduced fluorescence within the second window then may be the result of the lower intensity of the excitation beam.

We observed that the UV-burned "hole" can remain in the cell material for hours. We first exposed a fresh area of the cell to UV radiation at the horizontal position $X = 0$, and then moved the cell horizontally about 0.1 mm from the exposed area, and made a position scan in the X-direction continuously measuring the TL signal during the scan. The result of such scan is shown in Fig. 3(B). The X-scan shows a peak with FWHM of ~12 μm at $X = 0$. The peak width is close to the UV beam diameter determined by the beam profile measurement which is shown in Fig. 4(A). The plateau on both sides of the peak has the same low level as the initial signal on the unexposed area in Fig. 3(A). Two dips on both sides of the peak may be caused by the UV beam deflection by the local refractive index profile created by UV inscription. The X-scan was repeated twice, and the two scans gave almost identical profiles. The third scan made after the sample had been left unexposed overnight still demonstrated a very similar shape to that of the two first scans. From comparison of the three scans shown in Fig. 3(B) we have concluded that the damage of the cell window by UV radiation is permanent. The observed UV-induced inscription on the cell windows can certainly make the UV thermal lensing measurements with pulsed excitation not practical unless a method to avoid or at least to decrease it can be found.

The effects of irradiation of fused silica by pulsed UV beam with high-power and high-repetition rates, particularly for wavelengths shorter than 300 nm, have been studied in a number of publications which report loss of transparency and refractive index changes. It is believed that in the real fused silica glasses there always exist frozen-in intrinsic defects (e.g., stoichiometrically oxygen excess or deficient centers) which are possibly interconnected by mutual conversion reactions [25]. And these reactions can be stimulated by high intensity laser interaction. This conversion needs to be avoided in many cases such as high-precision UV photolithography. However, this effect can be turned to an advantage and used

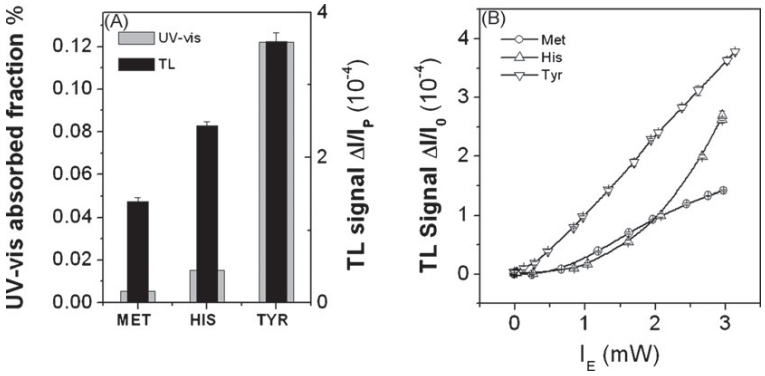

Fig. 5. (A) Comparison between linear absorption measurement by conventional UV–vis spectrometer at 266 nm and experimental TL signal for three representative amino acids, 10 mM methionine, 10 mM histidine and 0.05 mM tyrosine, at excitation UV power of 3 mW. The measured linear absorption coefficient is converted to be the fraction of UV power that is absorbed by the 100 μm sample layer. The TL signal of amino acid is subtracted by the background signal, i.e. signal with pure water. (B) Excitation power dependent background-subtracted TL signal for 10 mM methionine, 10 mM histidine and 0.05 mM tyrosine. Both figures have been recorded at the moderate focus condition.

to generate refractive index modulation in silica optical fibers for the fabrication of Bragg gratings [26].

Because the UV inscription rate is strongly dependent on UV power density, we studied the TL signal baseline behavior in time for different UV focusing conditions. The UV beam profiles for three focusing cases are shown in Fig. 4(A). As shown in Fig. 4(B) for loose and tight focusing cases the TL signal baseline remains virtually unchanged in contrast to the already studied case of moderate focusing. By looking at the beam profiles in Fig. 4(A), we can clearly see that moderate focusing provides the highest power density in the silica wall zones, therefore the most significant inscription rate. It is worth pointing out that the possible involvement of a TPA mechanism in UV inscription [26] may further amplify the difference in inscription rate among these focus conditions.

In the tight focusing case the TPA in the solvent may be much higher because of the energy concentration within the liquid, so the most promising operating condition for TL with pulsed UV beams may be loose focusing. However, the large beam diameter will then impair the TL applicability for the most interesting cases – small diameter capillaries or microchips. Consequently, the preferred operating condition for a given analyte volume is likely to involve tradeoffs.

3.4. Application of thermal lensing for the detection of amino acids

It is well known that only three aromatic amino acids, tyrosine, tryptophan, and phenylalanine, have strong absorption features near $\lambda = 266$ nm. For nonaromatic amino acids, the absorption at $\lambda = 266$ nm is weak. In this section our intent is to verify whether or not TPA can help in the detection of nonaromatic amino acids at this wavelength. Lack of data on TPA coefficients for amino acids makes difficult the predictions of the possible sensitivity of such TPA-assisted measurements, which means that we must measure them first. It turned out that TPA can result in a significant signal enhancement for some amino acids. We show in Fig. 5(A) a comparison between TL signals and the absorbed fraction of optical energy caused by linear absorption for three amino acids, tyrosine, methionine and histidine. The two nonaromatic AAs produce comparable TL signals to tyrosine that has a strong linear absorption at 266 nm, whereas their linear absorptions are significantly smaller. In order to verify that TPA is the origin of the large TL signals for nonaromatic AAs we studied the relationship between excitation power and TL signal. In Fig. 5(B), the power-dependent TL curves are subtracted from the background signal, i.e., the previously recorded TL signal from pure water. In accordance with our expectations, a linear dependence for tyrosine is observed, indicating that linear absorption dominates the TL signal. The TL signal for histidine has a quadratic dependence which confirms the two-photon absorption mechanism. The TL signal for methionine increases quadratically for low UV power values, but it starts to saturate above 1.5 mW. We suggest that photobleaching may be responsible for such saturation. We observed that nonpolar AAs (such as isoleucine, leucine, valine) have a higher tendency for TL signal saturation at high UV average powers.

As we have mentioned before, the relative contribution of linear absorption, TPA and UV inscription in the cell windows depends strongly on the focusing conditions. The inscription had virtually no effect for strong and loose focusing, whereas the TPA within the liquid sample should be emphasized for the strong focusing case. We measured therefore TL signals of 16 amino acids at different focusing conditions for the excitation laser. The results, which are illustrated in Fig. 5, show that some amino acids produce a TL signal that is clearly stronger than the background. The TL signal from pure water shown for comparison at the left in Fig. 5 increases monotonically as the focusing gets tighter as it should be for TPA. The signals for amino acids (with the background water signals subtracted) show complex behavior as a function of the UV laser focusing. Only some amino acids show a monotonic trend of increasing signal, such as lysine, serine, glutamine, arginine, and phenylalanine. Other amino acids show different kinds of uncorrelated trends (see Fig. 6). We assume this behavior is caused by the interplay of many factors as the focusing conditions change, such as the evolution from one-photon to two-photon absorption, and photodestruction/photochemical effects.

The complexity of observed effects increases with the energy density of the excitation beam which makes it difficult to use a potential advantage of the signal enhancement from the TPA. Our conclusion is that in order to advance the TL technique in small size capillaries further into the UV, special measures should be taken in order to decrease the energy density of the excitation UV beam both within the liquid probe volume and within the capillary material.

3.5. Capillary electrophoresis

Fig. 7 presents our preliminary results on separation of three native amino acids (tyrosine, tryptophan and cysteine) by capillary electrophoresis and TL detection. Full available power (8 mW on

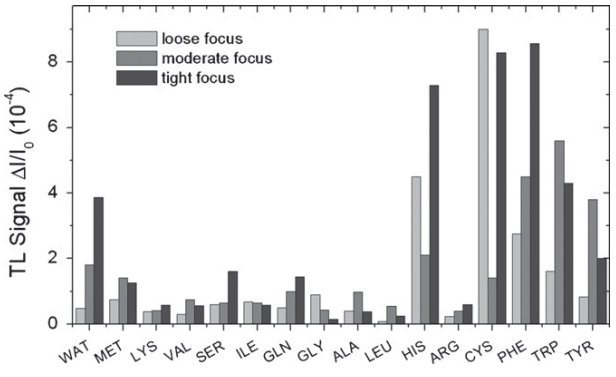

Fig. 6. TL signal of water and amino acid solutions (water signal subtracted) at different focus conditions of excitation laser. The average power of excitation laser is set at 4 mW. All amino acid solutions are prepared in pure water, with the concentrations of 10 mM, except for phenylalanine (500 mM), tryptophan (50 μM), and tyrosine (50 μM).

average) of the UV laser is used, and loose focusing is applied to decrease the UV energy density and unwanted nonlinear effects. Both square and round capillaries were tested. The baseline signal is primarily from TPA of the pulsed UV laser beam in the separation buffer (10 mM borate buffer at pH 9.3), which is very close to TPA in pure water. The baseline signal of 50 μm i.d. round capillary is about half of the 100 μm square in proportion with the two-fold UV beam path difference within the two capillaries. The peaks for all three amino acids can be clearly observed over the baseline variations. Some signal disturbances (short glitches) on the baseline originate from bubbles in the buffer and dust particles crossing the probe beam in this very preliminary experiment. Despite these glitches and despite the fact that no effort has been made in order to improve the stability of the UV beam, the detection limits look promising.

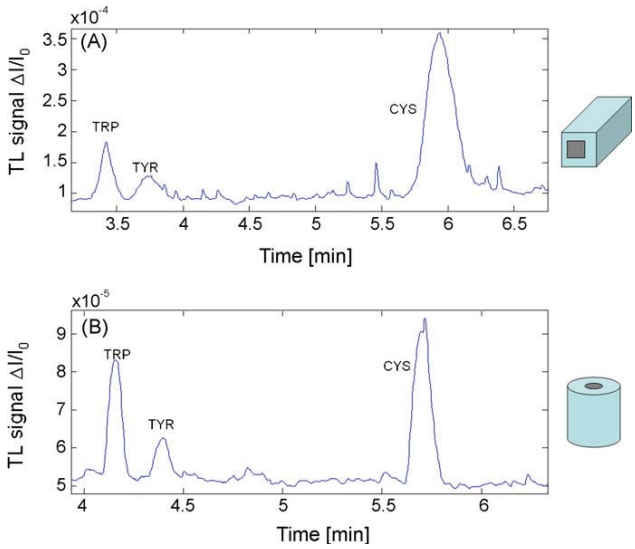

Fig. 7. Capillary electrophoresis separation of native amino acids. In (A), a 100 μm wide square, 30 cm capillary was used; the distance from the injector to the detector was 21 cm. The injection was 3.2 kV for 10 s. The separation proceeded at 5.2 kV. In (B), a 50 μm i.d., 50 cm long round capillary was used; the distance from the injector to the detector was 40 cm. The injection was 3.2 kV for 20 s. The separation proceeded at 13 kV. The mixture of the amino acid contains tryptophan 50 μM, tyrosine 50 μM, cysteine 1 mM. A 10 mM, pH 9.3 borate buffer was used both for the mixture solution preparation and the separation.

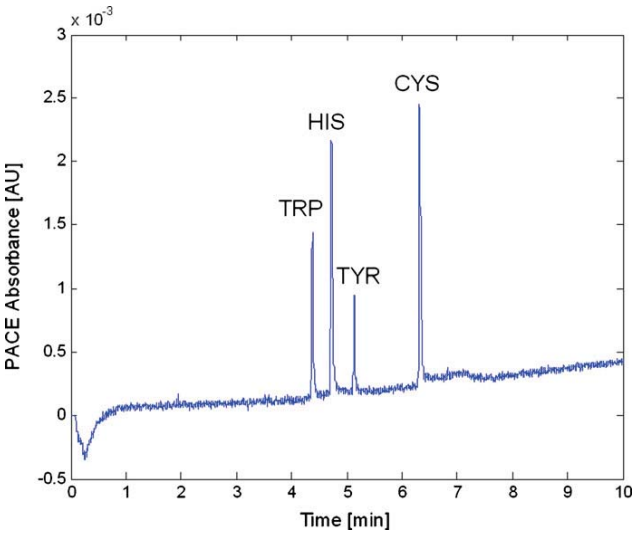

Fig. 8. Separation of several Amino Acids on PACE-200 at 214 nm. Experimental conditions: tryptophan (TRP) – 0.08 mM, histidine (HIS) – 0.8 mM, tyrosine (TYR) – 0.16 mM, cysteine (CYS) – 1.6 mM in 10 mM borate buffer, pH 10.1, capillary – 48/41 cm. ID 50 μm; separation voltage 14 kV, injection 1 s pressure.

The peak-to-peak baseline noise in Fig. 7(B) is $\sim 1.5 \times 10^{-6}$ AU. The signal-to-noise ratios for the TRP, TYR and CYS peak are 20, 7, and 30, which gives a minimum detectable concentration (MDC) of 2.5 μM, 7 μM and 33 μM, respectively.

Such limits of detection in concentration have been achieved across the capillary with a focused beam, which results in very low probe volume of only 140 pL. Accordingly, absolute limits of detection are 0.35 fmol for tyrosine, 0.125 fmol for tryptophan, and 1.65 fmol for cysteine.

For comparison, we made an attempt to detect several amino acids on a commercial CE system (Beckman PACE-2000) by measuring direct UV absorption across the same round capillary with 50 μm bore diameter. Fig. 8 shows the result of separation of four AAs at 214 nm – the shortest wavelength available with UV source in PACE-2000. We choose this option because no signals could be observed for nonpolar AAs at 266 nm with PACE and also because this wavelength is close to the fifth harmonics of Nd:YAG laser, and it can be obtained in a similar laser system to the one that we used on this experiment.

We can see that at this short wavelength there is a significant baseline drift in PACE; nevertheless, the peaks for all four AAs are clearly visible. The baseline noise in PACE for detection at 214 nm at 3σ level is 4.4×10^{-5} AU. From the peak heights for the individual amino acids in Fig. 8, we can determine the detection limits with PACE for TRP, TYR and CYS as 2.8 μM, 9.4 μM, and 32 μM, respectively. The detection limits in concentration with PACE are comparable to our results with TLS, but we should stress that the absorption coefficients for all three amino acids are significantly higher at 214 nm than at 266 nm, the wavelength we used for thermal lensing. This demonstrates again the potential of the TLS as an optical absorbance detector in separation technologies. If we compare the limits of detection in the absorbance units of both methods, we find out that TLS with pulsed excitation is about 30 times more sensitive than traditional CE based upon direct optical absorption measurement across the capillary. This makes a clear motivation to repeat these measurements with a similar source that emits at the fifth harmonics at 213 nm.

4. Conclusion

The UV TL method has been successfully applied to detect individual amino acids and a limited number of amino acids separated by CE. Unlabeled amino acids were detected because of their one-photon and two-photon absorption by pulsed 266 nm laser irradiation. The pulsed 266 nm laser source was compact and its size can be made close to the size of UV spectral lamps with housing and condenser that are commonly used in CE.

We also report several problems associated with using pulsed UV TL: (1) two-photon absorption of the solvent in pulsed UV TL brings significant background signal; (2) the fused silica material exhibits color center effects that interferes with the long-term stability of the baseline signal; and (3) possible photobleaching or photochemical destruction of the samples are involved. We found that these effects can be minimized by changing the focusing condition of the UV laser.

Acknowledgments

We are grateful to Dahv Kliner and Andrea Hansen from Sandia National Laboratories, Livermore, California for providing us the prototype 266 nm lasers system for their assistance in this work and valuable suggestions. F.Y. and R.N.Z. thank Skymoon Ventures Inc. for supporting this work.

References

[1] H.L. Fang, R.L. Swofford, in: D.S. Kliger (Ed.), Ultrasensitive Laser Spectroscopy, Academic Press, New York, 1983.
[2] N.J. Dovichi, Prog. Anal. Spectrosc. 11 (1988) 179.
[3] S.E. Bialkowski, in: J.D. Winefordner (Ed.), Photothermal Spectroscopy Methods for Chemical Analysis; Chemical Analysis, vol. 134, Wiley, New York, 1996.
[4] K. Abbas, J. Ghaleb, J. Georges, Spectrochem. Acta A 60 (2004) 2793.
[5] T.K.J. Pang, M.D. Morris, Anal. Chem. 56 (1984) 1467.
[6] T.G. Nolan, B.K. Hart, N.J. Dovichi, Anal. Chem. 57 (1985) 2703.
[7] F. Li, A.A. Kachanov, R.N. Zare, Anal. Chem. 79 (2007) 5264.
[8] J. Shen, D. Lowe, R. Snook, Chem. Phys. 165 (1992) 385.
[9] N.J. Dovichi, J.M. Harris, Anal. Chem. 51 (1979) 728.
[10] K.C. Waldron, N.J. Dovichi, Anal. Chem. 64 (1992) 1396.
[11] M. Chen, K.C. Waldron, Y. Zhao, N.J. Dovichi, Electrophoresis 15 (1994) 1290.
[12] K.C. Waldron, J. Li, J. Chromatogr. B 683 (1996) 47.
[13] X.F. Li, C.S. Liu, P. Roos, E.B. Hansen Jr., C.E. Cerniglia, N.J. Dovichi, Electrophoresis 19 (1998) 3178.
[14] B. Krattiger, A.E. Bruno, H.M. Widmer, R. Dandliker, Anal. Chem. 67 (1995) 124.
[15] N. Ragozina, S. Heissler, W. Faubel, U. Pyell, Anal. Chem. 74 (2002) 4480.
[16] S. Hiki, K. Mawatari, A. Hibara, M. Tokeshi, T. Kitamori, Anal. Chem. 78 (2006) 2859.
[17] J.J. Zayhowski, Rev. Laser Eng. 26 (1998) 841.
[18] S. Blackburn, Amino Acid Determination: Methods and Techniques, M. Dekker, 1968.
[19] J.T. Smith, Electrophoresis 20 (1999) 3078.
[20] http://www.mellesgriot.com/pdf/catalogx/x_01_27-28.pdf.
[21] T.I. Quickenden, J.A. Irvin, J. Chem. Phys. 72 (1980) 4416.
[22] A. Dragonmir, J.G. McInerney, D.N. Nikogosyan, Appl. Opt. 41 (2002) 4365.
[23] K.A. Ghaleb, J. Georges, Appl. Spectrosc. 60 (2006) 86.
[24] U. Natura, O. Sohr, R. Martin, M. Kahlke, G. Fasold, Proc. SPIE 5273 (2003) 155.
[25] L. Skuja, J. Non Cryst. Solids 239 (1998) 16.
[26] S.A. Slattery, D.N. Nikogosyan, G. Brambilla, J. Opt. Soc. Am. B 22 (2005) 354.